Computers Math. Applic. Vol. 26, No. 4, pp. 21–31, 1993
Printed in Great Britain.

0898-1221/93 $6.00 + 0.00

A Design Optimization Procedure for Efficient Turbine Airfoil Design

A. CHATTOPADHYAY, N. PAGALDIPTI AND K. T. CHANG
Department of Mechanical Engineering, Arizona State University
Tempe, AZ 85287-6106, U.S.A.

(Received September 1992; revised and accepted January 1993)

Abstract—An optimization procedure has been developed for the efficient design of turbine blade airfoil sections. A shape sensitivity study of the airfoils has been performed considering two leading edge shapes, circular and elliptic. Pressure and suction surfaces are approximated by polynomials. A two-level, nonlinear constrained optimization problem is formulated and is solved using the method of feasible directions. The aerodynamic analysis is performed using a two-dimensional panel code. Since several evaluations of the objective functions and the constraints are required within the optimizer, and exact aerodynamic analysis at each step is computationally prohibitive, a two-point exponential approximation technique has been used. The procedure developed successfully eliminates the sharp leading edge velocity spikes, characteristic of typical blade sections, without compromising blade performance. Circular leading edge airfoils appear to be more effective in eliminating the spikes than elliptic leading edge airfoils. However, the elliptic leading edge sections are more slender than the circular leading edge sections. Optimum results are compared with a reference design.

NOMENCLATURE

a_i	suction surface polynomial coefficients
a_{le}	semi-major axis of the leading edge ellipse
b_i	pressure surface polynomial coefficients
b_{le}	semi-minor axis of the leading edge ellipse
c_d	airfoil drag coefficient
c_l	airfoil lift coefficient
c_t	tangential force coefficient
mcp, x	meridional coordinate
n	degree of suction/pressure surface polynomials
r_b	radius of the turbine blade section
r_{le}	radius of the circular leading edge
t_k	thickness of the blade section at the k^{th} control point
x_{le}	meridional coordinate of the center of the leading edge circle/ellipse
x_m	m^{th} design variable
y	tangential coordinate
y_{le}	tangential coordinate of the center of the leading edge circle/ellipse
NCONT	total number of thickness control points
NCONV	total number of velocity control points
NDV	total number of design variables
NLED	total number of control points at the leading edge
V	objective function in Level 1 of the optimization
VG_i	velocity gradient at i^{th} velocity control point
ϕ	polar angle
β_1, β_2	leading edge angles defining the circular/elliptic arc
Ω	orientation of the semi-major axis of the leading edge ellipse
Subscripts	
l, min	lower bounds
u, max	upper bounds
le	pertaining to leading edge

Typeset by $\mathcal{A}_{\mathcal{M}}\mathcal{S}$-TEX

INTRODUCTION

A turbine design comprises three major steps [1]. The first is the determination of overall requirements of flow, work, and speed. The second is the evaluation of velocity diagrams, consistent with the desired efficiency. The last level is the design of the blade shape, size, and spacing of the blades. The blade chord length and the spacing are usually determined from solidity considerations. The design of blade shape involves the design of inlet and exit portions of the blade such that there is a smooth and efficient transition between the blade channel and the free stream with minimum loss. Consideration of the blade exit section includes the trailing edge, the throat, and the suction surface between the throat and the trailing edge. Design of the blade inlet section implies efficient design of the blade leading edge, which is the topic of interest here.

The leading edge geometry has long been treated as a less critical design criterion [2]. However, the leading edge geometry becomes critical for low reaction and high Mach number blading. In the case of low reaction blading, excessively high velocities in the inlet section can lead to high values of suction surface diffusion and a tendency toward increased losses. In the case of high inlet Mach numbers, area contraction leading to choking of the blade at the inlet must be avoided. The leading edges are associated with large curvatures which result in undesirable velocity spikes on both the suction and the pressure surfaces of the leading edge. Efficiency of turbo machinery blades can be greatly improved by eliminating these spikes. As indicated in [3], the leading edge heat transfer is also dependent on the blade shape. Since the maximum heat transfer occurs in the leading edge region, the magnitude of the reduction in heat transfer can be greatly increased by appropriate modification of the leading edge. Although circular leading edges are usually used in turbine blades, this specification is arbitrary and limits the freedom of the velocity distribution selection in the leading edge.

In spite of the important nature of the problem, very few formal investigations have been performed to investigate the effects of the leading edge shape variation on the turbine performance. In recent years, design optimization has become a practical tool which can expedite mechanical design. An extensive amount of work has been done in developing design optimization procedures to bring the state of the art to a very high level [4–6]. These techniques have received wide attention for fixed-wing aircraft designs [7–9] and are also being investigated recently for addressing various design issues in helicopter rotor blade design [10–15]. The use of numerical optimization procedures for the design of airfoils has been a subject of considerable interest, primarily for wing design [16–20]. The design problems addressed so far have been focussed on obtaining optimum airfoil shapes for maximizing or minimizing a prescribed design objective. For example, a two-dimensional inviscid aerodynamics program was coupled with an existing optimization algorithm for optimum airfoil design in [17,18] with the objectives of maximizing lift and minimizing drag. In [19], similar procedures were used for the design of a conventional windmill. Chung and Torres have developed a direct method to improve the C_l/C_d ratio of high speed wings [20]. With the knowledge available in the application of design optimization techniques, it is now of interest to investigate the problem of optimal shape design for turbine blades.

PROBLEM DESCRIPTION

Calculations of the flow field around the leading edge of the airfoil often show velocity spikes. The objective of this research is to develop an optimization procedure to eliminate the spikes without compromising blade performance. The tangential force coefficient of the turbine has been used as a measure of blade efficiency. First, an appropriate model is developed for the blade section. Next, a two-level, nonlinear constrained optimization problem is formulated. The parameters defining the shape of the blade are used as design variables during optimization.

BLADE MODEL

The blade section is modeled as shown in Figure 1. The suction surface (region BC) and the pressure surface (region DA) are approximated by polynomials of the form

$$y = a_0\sqrt{x} + a_1x + a_2x^2 + \cdots + a_nx^n, \tag{1}$$

where x is the meridional coordinate (mcp) and y is the tangential coordinate. The tangential coordinate is the product of the radius of the blade section (r_b) and the polar angle ϕ ($y = r_b * \phi$). Continuity of function and slope are imposed at junctions B and C for the suction surface polynomial and at junctions D and A for the pressure surface polynomial. These geometric requirements eliminate four coefficients from the set of independent variables in each of these polynomials. The remaining $n - 3$ coefficients (a_4 to a_n, Equation (1)) in each polynomial are used as design variables during optimization. Continuity of the second derivative is not imposed at the junctions because this requires that the surfaces be approximated by polynomials of higher order. These higher order polynomials seldom yield smooth aerodynamic shapes and approximate the surfaces poorly.

The leading edge shape is crucial in the current shape sensitivity study. Therefore, two leading edge models have been used. The circular leading edge model is illustrated in Figure 2 and is defined by the leading edge shape parameters, r_{le}, β_1, β_2, x_{le}, and y_{le}. The elliptic leading edge model is illustrated in Figure 3 and is defined by the leading edge shape parameters, a_{le}, b_{le}, β_1, β_2, Ω, x_{le}, and y_{le}. In both models, all leading edge parameters with the exception of x_{le} are used as design variables.

The trailing edge (region CD) is held fixed in order to satisfy the design requirement that the throat length of the turbine remain unaltered. The chord length of the airfoil section along the meridional direction is also held fixed. Since the trailing edge is fixed, this requires that the leading edge be tangential to the station $y = 0$ throughout the optimization ($y = 0$ being the tangential coordinate of the leading edge of the reference blade section). This tangency requirement determines x_{le}. In the case of circular leading edges,

$$x_{le} = r_{le}. \tag{2}$$

In the case of elliptic leading edges,

$$x_{le} = \sqrt{(a_{le}^2 \cos^2\Omega + b_{le}^2 \sin^2\Omega)}. \tag{3}$$

OPTIMIZATION FORMULATION

The objective of the optimization procedure is to reduce the velocity spikes near the blade leading edge without reducing the tangential force coefficient (C_t). The optimization problem is decomposed into two levels. A description of the two levels follows.

LEVEL 1. In this level, the objective function is the summation of the deviations of the velocity gradients, at several leading edge locations, from prescribed bounds. Constraints are imposed on the velocity gradient and the airfoil thickness at various chordwise locations. This level ensures a reduction in the leading edge velocity spikes and a possible elimination of the same.

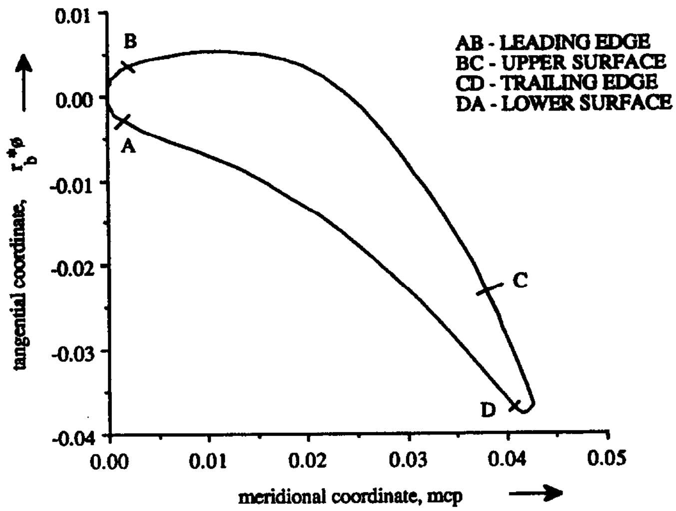

Figure 1. Blade model.

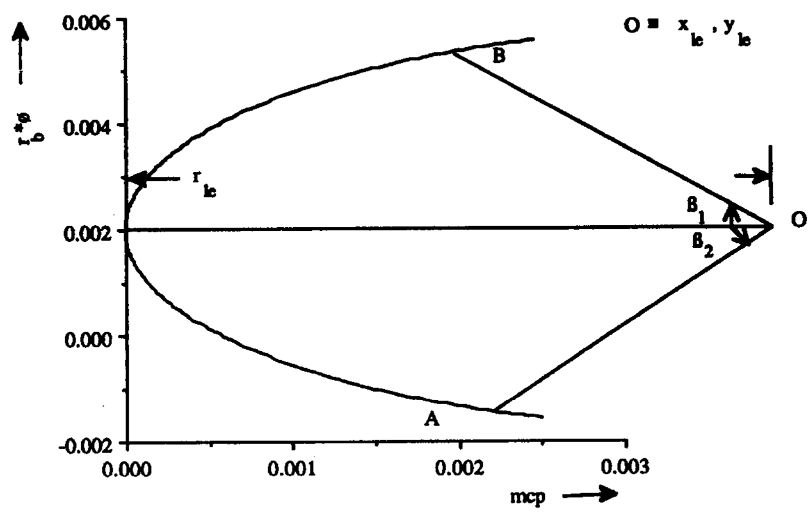

Figure 2. Circular leading edge model.

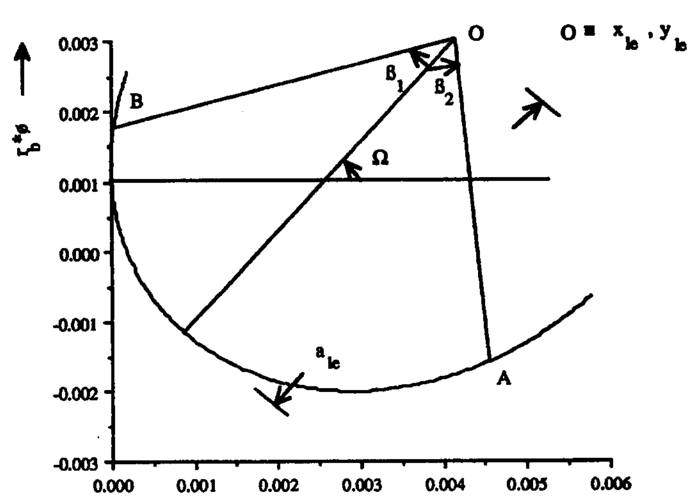

Figure 3. Elliptic leading edge model.

Mathematically, the problem can be stated as follows.

$$\text{Minimize} \quad \sum V_i \qquad i = 1, 2, \ldots, \text{NLED}$$

$$V_i = \begin{cases} VG_i - VG_{i_{\max}} & \text{if } VG_i > VG_{i_{\max}} \\ VG_{i_{\min}} - VG_i & \text{if } VG_i < VG_{i_{\min}} \\ 0 & \text{otherwise} \end{cases}$$

$$\begin{aligned} VG_i &= \text{Velocity gradient at } i^{\text{th}} \text{ leading edge control point} \\ VG_{i_{\max}} &= \text{Prescribed upper bound for velocity gradient} \\ &\quad\ \text{at } i^{\text{th}} \text{ leading edge control point} \\ VG_{i_{\min}} &= \text{Prescribed lower bound for velocity gradient} \\ &\quad\ \text{at } i^{\text{th}} \text{ leading edge control point} \\ \text{NLED} &= \text{Total number of leading edge locations} \end{aligned}$$

subject to

$$\begin{aligned} &VG_j \le VG_{j_{\max}} && j = 1, 2, \ldots, \text{NCONV} \\ &VG_j \ge VG_{j_{\min}} && j = 1, 2, \ldots, \text{NCONV} \\ &t_k \le t_{k_{\max}} && k = 1, 2, \ldots, \text{NCONT} \end{aligned}$$

$$\begin{aligned} t_k &= \text{Thickness of the airfoil section at } k^{\text{th}} \text{ control point} \\ t_{k_{\max}} &= \text{Prescribed upper bound on the airfoil thickness} \\ &\quad\ \text{at } k^{\text{th}} \text{ control point} \\ \text{NCONV} &= \text{Total number of chordwise velocity control points} \\ \text{NCONT} &= \text{Total number of chordwise thickness control points} \end{aligned}$$

and

$$x_{ml} \le x_m \le x_{mu} \qquad m = 1, 2, \ldots, \text{NDV (side constraints)}$$

$$\begin{aligned} \text{NDV} &= \text{Total number of design variables} \\ x_m &= m^{\text{th}} \text{ design variable.} \end{aligned}$$

LEVEL 2. The objective function in this level is the tangential force coefficient (C_t). Constraints are imposed on the velocity gradients such that their values remain close to those obtained from Level 1. Mathematically, the problem is stated as follows.

Maximize Tangential force coefficient (C_t)

subject to

$$\begin{aligned} &VG_j \le VG_{j_{\max_1}} && j = 1, 2, \ldots, \text{NCONV} \\ &VG_j \ge VG_{j_{\min_1}} && j = 1, 2, \ldots, \text{NCONV} \\ &t_k \le t_{k_{\max}} && k = 1, 2, \ldots, \text{NCONT} \end{aligned}$$

$$\begin{aligned} VG_{j_{\max_1}} &= \text{Upper bound on the velocity gradient} \\ &\quad\ \text{at } j^{\text{th}} \text{ velocity control point based} \\ &\quad\ \text{on the value obtained in Level 1} \\ VG_{j_{\min_1}} &= \text{Lower bound on the velocity gradient} \\ &\quad\ \text{at } j^{\text{th}} \text{ velocity control point based} \\ &\quad\ \text{on the value obtained in Level 1} \end{aligned}$$

and

$$x_{ml} \le x_m \le x_{mu} \qquad m = 1, 2, \ldots, \text{NDV (side constraints).}$$

Side constraints are imposed on the design variables in both levels to avoid unrealistic designs. The subscripts l and u denote lower and upper bounds, respectively, on the design variables, imposed to constrain the design in a practical range. NDV is the total number of design variables.

OPTIMIZATION IMPLEMENTATION

A gradient based optimization technique, which is based on the method of feasible directions, has been used to solve the nonlinear programming problem [21]. Sensitivity analysis is performed using the finite difference method. Exact aerodynamic analysis is performed using a two-dimensional panel code developed by McFarland [22]. Since the optimization process requires many evaluations of the objective function and the constraints before an optimum design is obtained, the process can be very expensive if actual aerodynamic analyses are performed for each function evaluation. The objective function and constraints are therefore approximated by a two-point exponential approximation [23] based on the design variable values from the optimizer and the sensitivity information from the aerodynamic analyses. The method has been found to provide good approximations in highly nonlinear constrained optimization problems [14]. Specifically, if a function F and its derivatives are calculated for the design X_0, its value for a new design X_n is given by

$$f(X_n) = f(X_0) + \sum_{i=1}^{\mathrm{NDV}} \left(\left(\frac{x_{ni}}{x_{0i}} \right)^{p_i} - 1 \right) \frac{x_{0i}}{p_i} \frac{\partial F}{\partial x_i}(X_0), \tag{4}$$

where F is the function that is being approximated, X_0 is the old design vector, X_n is the new design vector, x_i is the i^{th} design variable, x_{0i} is the i^{th} design variable of the old design vector, x_{ni} is the i^{th} design variable of the new design vector, p_i is the parameter controlling the approximation, and NDV is the total number of design variables. For $p_i = 1$, the approximation reduces to a first order Taylor expansion. For $p_i = -1$, the approximation reduces to a reciprocal Taylor expansion. A move limit, typically defined as the maximum fractional change of each design variable value, is imposed as upper and lower bounds on each design variable x_i.

RESULTS

The optimization procedure is applied to several airfoils which are based on the test blade section given in [22]. Both circular and elliptic leading edge airfoils have been considered. The two-level optimization procedure is very effective in eliminating the leading edge spikes without affecting its performance. The two-point approximation used within the optimizer is sufficiently accurate, and procedure converges to the optimum design within 15 cycles. Representative results from two cases are presented here.

Case 1—Circular Leading Edge

The airfoil section is modeled with a circular leading edge. The reference and the optimum airfoil shape parameters are presented in Tables 1–3. Table 1 gives the leading edge shape parameters. The radius of the leading edge circle of the optimum blade is reduced by 5.25%. The upper leading edge angle (β_1) for the optimum blade is decreased by 7.6%, whereas the decrease in the lower leading edge angle (β_2) is 2.1%. The meridional coordinate of the leading edge circle center changes with the radius of the leading edge. This maintains the tangency of the leading edge to the station, mcp = 0. There is also a significant increase in the tangential coordinate of the leading edge circle center.

Tables 2–3 give the suction and the pressure surface polynomial coefficients. Fifth order polynomials have been used to model these surfaces. Four of the six coefficients in each polynomial are fixed by continuity and differentiability requirements on the polynomial at the leading edge and trailing edge junctions. The coefficients a_4 and a_5 are used as design variables from the

Table 1. Leading edge shape parameters (5^{th} degree polynomial), Case 1.

Leading Edge Shape Parameters	Reference Blade	Optimum Blade
Radius (m)	0.00381	0.00361
β_1 (deg)	61.3	56.62
β_2 (deg)	27.6	27.03
x_{le}	0.00381	0.00361
y_{le}	0.0	0.00025

Table 2. Suction surface polynomial (5^{th} degree polynomial), Case 1.

Suction Surface Polynomial Coefficients	Reference Blade	Optimum Blade
a_0	0.12292	0.12543
a_1	−1.3587	−1.3373
a_2	166.694	163.782
a_3	−12455.16	−12397.56
a_4	379474.7	379474.7
a_5	−4525559.2	−4525559.2

Table 3. Pressure surface polynomial (5^{th} degree polynomial), Case 1.

Pressure Surface Polynomial Coefficients	Reference Blade	Optimum Blade
b_0	−0.08836	−0.06074
b_1	0.1338	−0.5185
b_2	92.349	115.842
b_3	−9013.22	−9279.32
b_4	251168.6	251168.6
b_5	−2319274.5	−2319274.5

Table 4. Leading edge shape parameters (4^{th} degree polynomial), Case 2.

Leading Edge Shape Parameters	Reference Blade	Optimum Blade
Semi-major axis (m)	0.00420	0.00612
Semi-minor axis (m)	0.00336	0.00480
β_1 (deg)	61.3	68.21
β_2 (deg)	47.6	48.57
Ω (deg)	0.0	−0.18172
x_{le}	0.00420	0.00612
y_{le}	0.00150	0.00185

Table 5. Suction surface polynomial (4^{th} degree polynomial), Case 2.

Suction Surface Polynomial Coefficients	Reference Blade	Optimum Blade
a_0	0.15640	0.17218
a_1	−1.3920	−1.1956
a_2	38.558	15.749
a_3	−518.22	−73.20
a_4	−17722.6	−17759.9

Table 6. Pressure surface polynomial (4^{th} degree polynomial), Case 2.

Pressure Surface Polynomial Coefficients	Reference Blade	Optimum Blade
b_0	−0.01441	−0.02218
b_1	−0.3698	−0.4038
b_2	14.323	18.771
b_3	−1168.02	−1244.47
b_4	13156.4	13425.04

suction surface polynomial. Similarly, coefficients b_4 and b_5 are used as design variables from the pressure surface polynomial. There are considerable changes in the values of the coefficients of the suction surface polynomial, a_0 through a_3, and the coefficients of the pressure surface polynomial, b_0 through b_3. However, the changes in the values of the coefficients, a_4, a_5, b_4, and b_5, are insignificant. This clearly indicates that increasing the degree of the approximating polynomials does not help the design procedure significantly. Also, higher degree polynomials are highly nonlinear and have been found to produce undesired shapes.

Figure 4 shows the reference and the optimum airfoils. There is a significant increase in the leading edge thickness as shown by the figure. Figures 5 and 6 show the velocity distributions for the reference and the optimum blades as a function of the meridional coordinate. These figures indicate that the leading edge spikes have been eliminated. The tangential force coefficient is maintained at the reference design value. This indicates that the design procedure does not compromise on blade performance and maintains it close to the reference value.

Case 2—Elliptic Leading Edge

The airfoil is modeled with an elliptic leading edge. The reference and the optimum airfoil section shape parameters are presented in Tables 4–6. Table 4 gives the leading edge shape

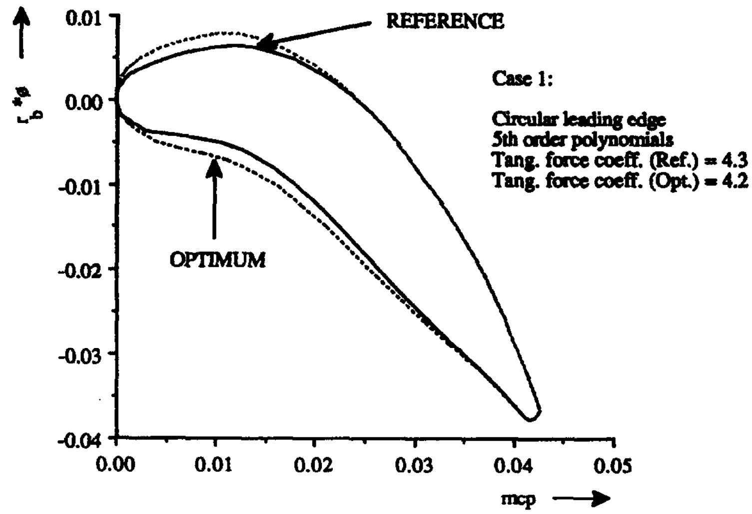

Figure 4. Airfoil shape, Case 1.

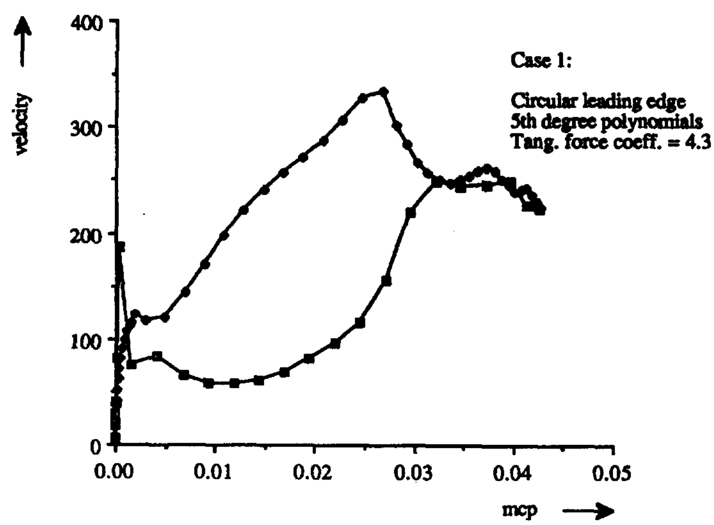

Figure 5. Reference blade velocity distribution.

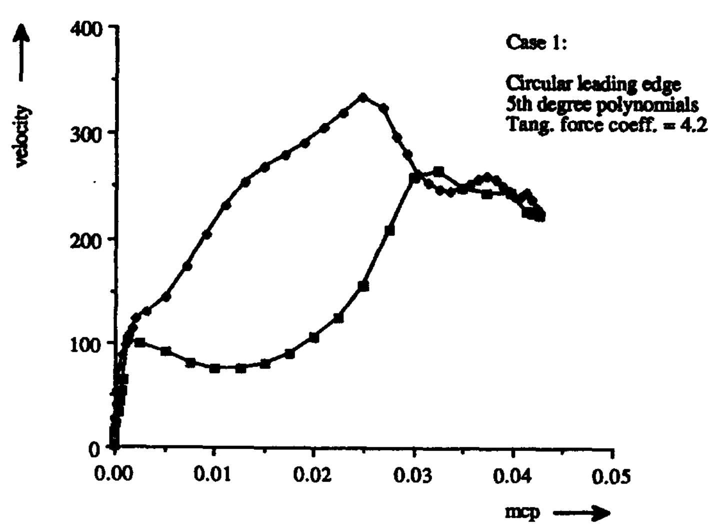

Figure 6. Optimum blade velocity distribution.

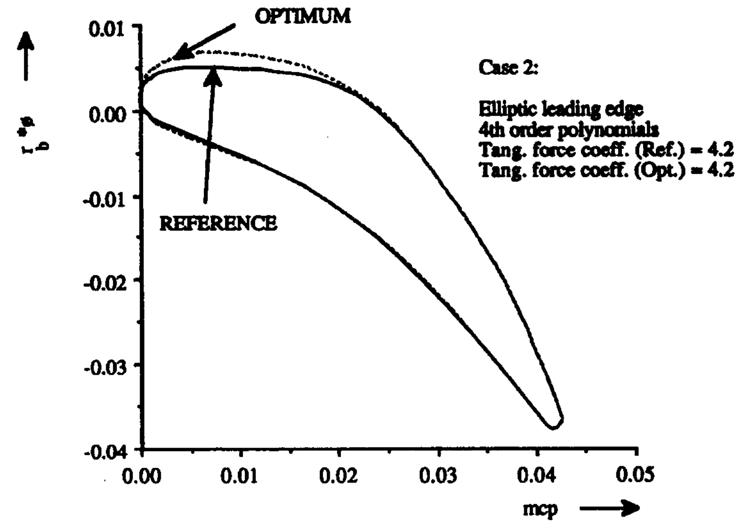

Figure 7. Airfoil shape, Case 2.

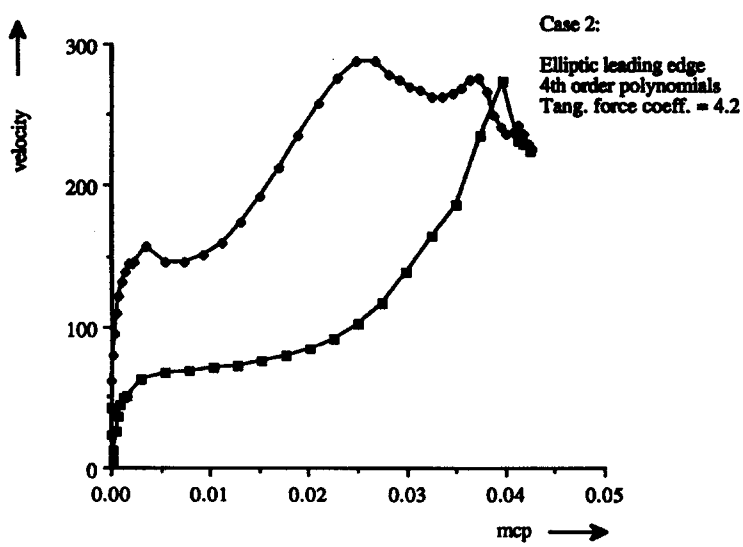

Figure 8. Reference blade velocity distribution.

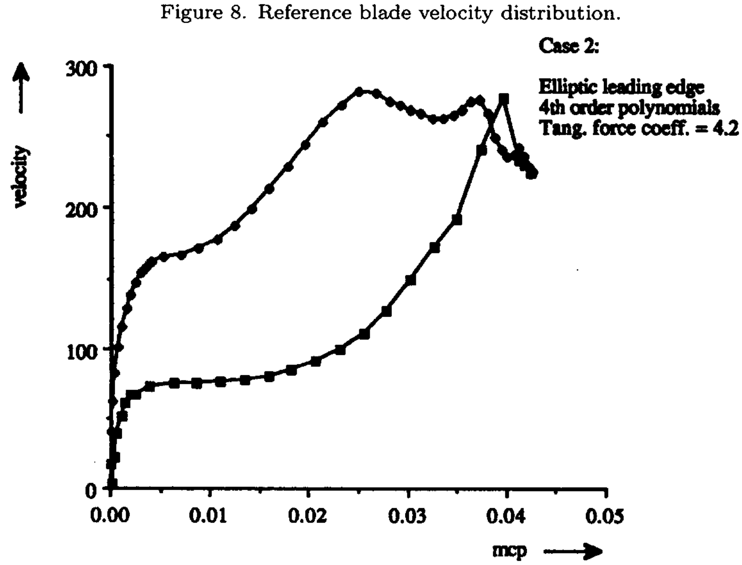

Figure 9. Optimum blade velocity distribution.

parameters. There are significant increases in all the leading edge shape parameters in this case unlike the circular leading edge case. The semi-major axis is increased by 45.7%, and the semi-minor axis is increased by 42.9%. The upper leading edge angle is also increased significantly (11.3%). The meridional coordinate of the leading edge center (x_{le}) changes in accordance with the tangency requirement. Fourth order polynomials are used for the suction and the pressure surfaces. Tables 5 and 6 present the polynomial coefficients. The changes in the values of the higher order coefficients are small, which follows the observation in Case 1. The changes in the remaining coefficients are more pronounced in this case than in the circular leading edge case.

Figure 7 shows the reference and the optimum blades. It can be seen that the change in the leading edge thickness is not as significant as in the previous case (circular leading edge) where the thickness increases considerably. Slenderness of the blade is maintained. Figures 8 and 9 show the velocity distributions for the reference and the optimum blades. The leading edge spikes are eliminated successfully in the optimum blades, as can be seen from these figures.

The time saved by using an approximate analysis inside the optimizer depends on the number of design variables, the time required for each exact analysis, and the number of approximate steps allowed before an exact solution is required to check the accuracy of the approximation. For the problem under consideration, the number of design variables is between four and eight for circular leading edge model, and between six and ten for elliptic leading model. The time required for an exact analysis is about 0.3 cpu seconds on the CRAY-XMP and the number of approximate steps allowed before an exact solution averages to four. Therefore, the time saved using the approximate analysis ranges between 5 to 15 cpu seconds (20% to 50% of the actual run time). For cpu intensive problems, the time saved using the approximate analysis can be significant.

CONCLUDING REMARKS

An optimization procedure has been developed for efficient design of turbine blades. The procedure developed successfully eliminates the spikes without affecting blade performance. The following observations are made based on the various cases studied.

1. The two-level optimization procedure is very effective in designing airfoils for turbines. The procedure converges to the optimum within an average of 15 cycles.
2. Circular leading edge airfoils are more effective in eliminating the spikes than elliptic leading edge airfoils.
3. Optimum elliptic leading edge sections are more slender than the optimum circular leading edge sections.
4. The two-point approximation used along with the optimizer reduces CPU time significantly and is sufficiently accurate.

REFERENCES

1. A.J. Glassman, Turbine design and applications, *NASA SP 290* **1,2** (1972).
2. W.L. Stewart and A.J. Glassman, Blade design, Chapter 4, *NASA SP 290* **2** (1972).
3. K.C. Civinskas, Impact of ETO propellents on the aerothermodynamic analyses of propulsion components, *AIAA/ASME/SAE/ASEE 24th Joint Propulsion Conference*, Paper No. AIAA 83-3091, Boston, Massachusetts, (July 1988).
4. H. Ashley, On making things the best—Aeronautical use of optimization, *AIAA Journal of Aircraft* **19** (1) (1982).
5. J. Sobieszczanski-Sobieski, Structural optimization challenges and opportunities, *Int. Conf. on Modern Vehicle Design Analysis*, London, England, (June 1983).
6. J. Sobieszczanski-Sobieski, Recent experiences in multidisciplinary analysis and optimization, *NASA CP-2327* (1984).
7. J. Sobieszczanski-Sobieski, Sensitivity analysis and multidisciplinary optimization for aircraft design: Recent advances and results, *16th Congress of the Int. Council of Aeronautical Sciences*, Paper ICAS-99-1.7.3, pp. 953–964, Jerusalem, Israel, (August–September 1988).

8. S.M. Dollyhigh and J. Sobieszczanski-Sobieski, Recent experiences with multidisciplinary analysis and optimization in advanced aircraft design, *Proc. 3rd Airforce/NASA Symp. on Recent Advances in Multidisciplinary Analysis and Optimization*, San Fransisco, California, (September 1990).
9. J.F.M. Barthelemy, P.G. Coen, G. Wrenn, M.F. Riley and A.R. Dovi, Application of multidisciplinary optimization methods to the design of a supersonic transport, *Proc. 3rd Airforce/NASA Symp. on Recent Advances in Multidisciplinary Analysis and Optimization*, San Fransisco, California, (September 1990).
10. P.P. Friedman, Application of modern structural optimization to vibration reduction in rotorcraft, *Vertica* **9** (4), 363–373 (1985).
11. A. Chattopadhyay and J.L. Walsh, Minimum weight design of rectangular and tapered helicopter rotor blades with frequency constraints, *Proc. 2nd Int. Conf. on Rotorcraft Basic Research*, College Park, Maryland, (February 1988); *Journal of the AHS*, (October 1989).
12. A. Chattopadhyay and J.L. Walsh, Minimum weight design of rotorcraft blades with multiple frequency and stress constraints, *Proc. AIAA/ASME/ASCE/AHS 29th Structures, Structural Dynamics and Materials Conference*, Williamsburg, Virginia, (April 1988); *AIAA Journal*, Paper No. 88-2337-CP, (March 1990).
13. A. Chattopadhyay, J.L. Walsh and M.F. Riley, Integrated aerodynamic/dynamic optimization of helicopter blades, *Proc. AIAA/ASME/ASCE/AHS 30th Structures, Structural Dynamics and Materials Conference*, Mobile, Alabama, (April 1989); Special Issue of the *AIAA J. of Aircraft*, Paper No. 89-1269, (January 1991).
14. A. Chattopadhyay and T.R. McCarthy, Multiobjective design optimization of helicopter rotor blades with multidisciplinary couplings, *Proc. OPTI91—Computer Aided Optimum Design of Structures*, Boston, Massachusetts, (June 1991).
15. Y.D. Chiu and A. Chattopadhyay, Aerodynamic sensitivity derivatives of rotary wings in axial flight, *Proc. 3rd Airforce/NASA Symp. on Recent Advances in Multidisciplinary Analysis and Optimization*, San Fransisco, California, (September 1990).
16. D.S. Hague, H.L. Rozendaal and F.A. Woodward, Application of multivariable search techniques to optimal aerodynamic shaping problems, *Journal of Astronautical Sciences* **15** (6), 283–296 (November–December 1968).
17. G.N. Vanderplaats, R.M. Hicks and E.M. Murman, Application of numerical optimization techniques to airfoil design, *Proc. Aerodynamic Analyses Requiring Advanced Computers*, Vol. II, Langley Research Center, Hampton, Virginia, (March 1975).
18. G.N. Vanderplaats and R.M. Hicks, Numerical airfoil optimization using a reduced number of design coordinates, *NASA TMX-73* **151** (July 1976).
19. G.N. Vanderplaats and A.E. Fuhs, Aerodynamic design of a conventional windmill using numerical optimization, Technical Note, *J. of Energy* **1** (2), 132–134 (March–April 1977).
20. I. Chung Chang and F.J. Torres, Wing design code using three dimensional Euler equations and optimization, *AIAA Aircraft Design Systems and Operations Meeting* (September 1991).
21. G.N. Vanderplaats, CONMIN—A FORTRAN program for constrained function minimization, Users' Manual, *NASA TMX-62282* (July 1987).
22. E.R. McFarland, Panel code for 2D blade to blade solutions, *NASA TMX-81589*.
23. G.M. Fadel, M.F. Riley and J.F. Barthelemy, Two-point exponential approximation method for structural optimization, *Structural Optimization* **2**, 117–124 (1990).